

1 **Climate change projections of**
2 **medicanes with a large multi-model**
3 **ensemble of regional climate**
4 **models**

5 Raquel Romera^{a,e}, Miguel Ángel Gaertner^{b,f}, Enrique Sánchez^{b,g}, Marta Domínguez^c, Juan Jesús
6 González-Alemán^{a,h} and Mario Marcello Miglietta^{d,i}

7 ^aEnvironmental Sciences Intitute, University of Castilla-La Mancha, 45071 Toledo, Spain

8 ^bEnvironmental Sciences Faculty, University of Castilla-La Mancha, 45071 Toledo, Spain

9 ^cDepartamento de Física de la Tierra, Astronomía y Astrofísica I (Geofísica y Meteorología),
10 Physics Sciences Faculty, University Complutense of Madrid, Madrid, Spain

11 ^dConsiglio Nazionale delle Ricerche, Istituto di Scienze dell'Atmosfera e del clima, 73100 Lecce,
12 Italy

13 ^eRaquel.Romera@uclm.es (corresponding author)

14 ^fMiguel.Gaertner@uclm.es

15 ^gE.Sanchez@uclm.es

16 ^hJuanJesus.Gonzalez@uclm.es

17 ⁱm.miglietta@isac.cnr.it

18 **Abstract**

19 Cyclones with tropical characteristics, usually called medicanes, occasionally develop over the
20 Mediterranean Sea. Possible future changes of medicanes are a matter of concern due to their large
21 damage potential. Here we analyse a large set of climate change projections with regional climate
22 models (RCMs) from ENSEMBLES project. The aim is to increase our knowledge about the future
23 evolution of medicanes, advancing previous studies along several important lines: use of a large
24 ensemble of RCMs, nested in many different GCMs, and covering a long continuous time period
25 (up to 150 years). The main overall results are a future reduction in the number of medicanes and an
26 increase in the intensity of the strongest medicanes, in agreement with other studies. But the large
27 size of the ensemble reveals some important model-related uncertainties. The frequency decrease is
28 not statistically significant in many of the simulations extending to 2100, with two simulations even
29 showing no frequency decrease at all. Large decadal changes affect the medicane frequency,
30 emphasizing the need for long period simulations. The increase in extreme intensity shows a clear
31 dependence on the GCM driving the simulations. In contrast to the overall results, a few simulations
32 also show changes in the monthly distribution of medicanes, with less winter cases and more
33 autumn and late summer cases. Some environmental variables have been explored in an attempt to
34 offer physical explanations for these results. A plausible reason for the overall decrease of medicane
35 frequency is the projected increase in vertical static stability of the atmosphere. A relevant result is
36 that the general and clear increase in average static stability is unable to avoid that several
37 simulations project higher maximum winds in the future. This could indicate that the increased SST
38 and latent heat fluxes may overcome the limitation of a higher overall static stability, if favourable
39 conditions for medicane genesis indeed occur. This is a worrying possibility, as the strongest
40 damages are associated to the most intense cyclones.

41

42 **Keywords:** Medicanes, Climate Change, Mediterranean cyclones, Regional Climate Models

43 **1.1 Introduction**

44 The Mediterranean Sea is a region with a high density of cyclones (more than 1500 cyclones/year
45 according to Campins et al., 2011), which are responsible for heavy precipitation and strong wind
46 events (Jansá et al., 2001; Bocheva et al., 2007; Trigo et al., 2000; Nissen et al., 2010).

47 Mediterranean cyclones are often responsible for considerable damages mainly in the
48 Mediterranean islands and coastal zones, due to their greater exposure to strong winds and floods. A
49 better understanding and description of these extreme meteorological phenomena in the present
50 climate can be crucial to understand and predict the response of the Mediterranean climate to global
51 climate change during the current XXIst century.

52 Not all the Mediterranean cyclones have the same characteristics: some recent studies have focused
53 on cyclones with tropical characteristics (axial thermal symmetry and warm core) over the
54 Mediterranean Sea, the so called medicanes (acronym for Mediterranean Hurricanes). The singular
55 situation of the Mediterranean Sea favours the development of such tropical-like cyclones. Gibraltar
56 Strait is the only communication with the Atlantic Ocean so the water exchange is very limited and
57 the Mediterranean water temperature may reach very high values in September. Another special
58 feature of the Mediterranean Sea is the surrounding orography: high mountains like the Alps
59 surround the basin and modify the circulation, favouring the generation of baroclinic cyclones,
60 which later may develop into medicanes.

61 Different studies have shown that medicanes do not happen in all locations of the Mediterranean
62 Sea with the same probability. In the climatological studies by Tous and Romero (2013) and
63 Cavicchia et al. (2014a), the same two preferred regions of occurrence came out (Ionian Sea and
64 Balearic Islands), although the methodology they used was based in the former case on satellite
65 images and in the latter on numerical simulations. The combined satellite and numerical approach
66 uses in Miglietta et al. (2013) identified fourteen medicanes among the cases described in the
67 literature and in the websites from 1999 to 2012, reproducing a similar geographic distribution.

68 From a modelling perspective, the use of General Circulation Models (GCMs) to analyse medicanes
69 is not possible due to the typical size of the medicanes and the low resolution of GCMs, as
70 medicanes have typically a diameter of less than 300 km (Walsh et al., 2014). Therefore, the use of
71 higher resolution models, such as Regional Climate Models (RCMs), is necessary. Chapter 14 of the
72 last IPCC report (Christensen et al., 2013) pointed out the important spread among the cyclones
73 detected by different RCMs, which is similar to the changes expected in the future scenarios or to
74 the natural interannual variability. The use of a model ensemble allows to take into account the large
75 spread among different climate models, which represents an added value in comparison with studies
76 using only one RCM (e.g. Walsh et al., 2014; Cavicchia et al., 2014b).

77 Gaertner et al. (2007) used an ensemble of RCMs from PRUDENCE European project
78 (Christensen and Christensen, 2007), with a grid spacing of 50 km, to analyse projections of future
79 intense cyclones over the Mediterranean Sea. That study detected for the first time a future risk of
80 tropical cyclone development over the Mediterranean Sea, and stressed the need for higher
81 resolution and a more complete ensemble of RCMs (higher number of RCMs, use of different
82 GCMs or different emission scenarios). It is expected that the number of detected cyclones may
83 increase using higher resolution models, as smaller cyclones could be missed if the resolution used
84 is too coarse (Pinto et al., 2005). ENSEMBLES project (Van der Linden and Mitchell, 2009)
85 extended the analysis from PRUDENCE increasing the number of RCMs, the number of GCMs,
86 and reducing the horizontal grid spacing (25 km). The simulated period was also much larger than
87 in PRUDENCE.

88 The present study aims to analyse climate change projections of medicanes, advancing previous
89 studies along several important lines: use of a large ensemble of RCMs, nested in several different
90 GCMs, and covering a long time period (up to 150 years). These are advantages of ENSEMBLES
91 project compared to PRUDENCE. First, the ERA40 forced simulations for 1961-2000 period are
92 evaluated against the available observational information about medicanes to determine the
93 capability of these RCMs to describe the observed characteristics. Then, both present (1951-2000)

		RCM (Institution)								
		RCA3 (C4I)	ALADIN (CNRM)	CLM (ETHZ)	HadRM3Q16 (HC)	HadRM3Q3 (HC)	RACMO (KNMI)	HIRHAM (METNO)	REMO (MPI)	RCA (SMHI)
	BCM						A1B 1951-2050		A1B 1961-2100	
	HCQ0			A1B 1951-2099			A1B 1951-2050			A1B 1951-2050
	HCQ16				A1B 1951-2099					
	HCQ3					A1B 1951-2099			A1B 1951-2100	

111 Table 1: Summary of models, institutions, periods and scenarios used in the present study.

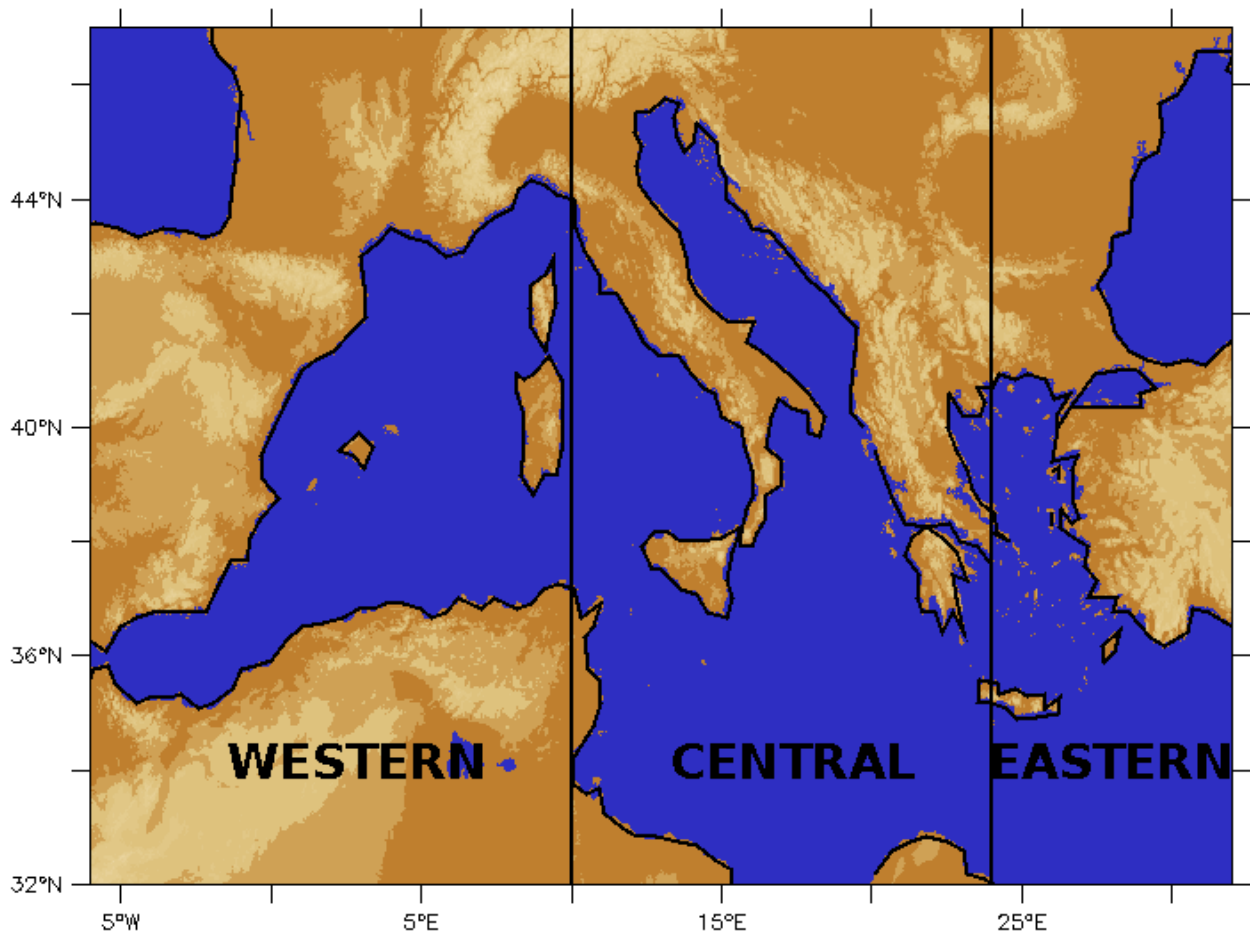
112 The Mediterranean Sea has been divided in three zones (see Figure 1) in order to study the regional
113 distribution of medicanes: Western (longitude less than 10°E), Central (longitude greater than 10°E
114 and less than 24°E) and Eastern (longitude greater than 24°E). Those subregions are comparable to
115 the ones described in Giorgi and Lionello (2008). Here, the cyclones are assigned to a subregion
116 when they reach their maximum intensity as a medicane.

117 1.2.1 Cyclone Detection Method

118 The cyclone detection method described by Picornell et al. (2001) based on sea level pressure (SLP)
119 has been used. August to January daily SLP averages are analysed to identify the pressure minima.
120 A Cressman filter with a radius of 200 km is next used (Sinclair, 1997) to smooth out noisy features
121 appearing in the SLP field. Weaker cyclones are filtered out through a SLP gradient threshold, and a
122 radius of 400 km around every SLP minimum is used for determining the cyclone extension.

123 The cyclone tracks have been calculated using the horizontal wind at 700 hPa as an auxiliary
124 variable indicating the likely direction of movement of the cyclones. A 10 m wind filter has been
125 applied, dismissing all the cyclones whose daily maximum 10 m wind speed is less than 17.5 m·s⁻¹
126 during their whole lifetime, as that value is the threshold to distinguish between a tropical

127 depression and a tropical storm (or the threshold for gale force in the Beaufort Scale).



128 Figure 1: Topography of the studied domain and subregions chosen for the study.

129 1.2.2 Vertical Structure of the Cyclones (Medicanes classification)

130 The geopotential fields between 900 and 300 hPa have been used to apply the cyclone phase space
131 method (Hart, 2003) in order to select the medicanes among all the detected cyclones. The Hart
132 method is based on three parameters: B , $-V_T^U$ and $-V_T^L$. The B parameter is a measurement of the
133 symmetry or asymmetry of the cyclone; a value of B near zero indicates that the cyclone is
134 symmetric, with 10 m being a suitable threshold below which symmetric cyclones are identified
135 (following Hart, 2003). $-V_T^L$ (lower troposphere thermal wind) and $-V_T^U$ (upper troposphere
136 thermal wind) parameters determine the existence of a warm or cold core between 900 and 600 hPa
137 ($-V_T^L$) and between 600 and 300 hPa ($-V_T^U$). Tropical cyclones show a full-troposphere warm core,
138 and thus $-V_T^L$ and $-V_T^U$ must both be positive (Hart, 2003).

139 In this study all the cyclones with $-V_T^L$ above zero and $-V_T^U$ greater than -10 m are selected as
140 medicanes. The latter threshold of -10 m has been chosen to include also some cyclones showing an
141 upper tropospheric warm core during less than one day, as the data used here are daily average
142 values. The parameters have been calculated using a radius of 150 km, chosen as representative of
143 the typical dimension of medicanes. B parameter has been calculated when possible. However, it
144 cannot be calculated with daily values for cyclones with 1 day lifetime, as the direction of
145 movement of the cyclone is needed. Due to this, B has not been used in the selection of medicanes.

146 **1.3 Results**

147 **1.3.1 RCM evaluation against available observations**

148 From a purely observational point of view, it is difficult to detect medicanes from surface
149 measurements, as many of them do not touch the coastline and ships try to avoid them. With the use
150 of satellites it has been possible to create a list of observed events but this is limited to the recent
151 past so it is impossible to know the frequency of medicanes further back in time. Some studies have
152 estimated that the frequency of the medicanes is one or two events per year (Romero and Emanuel,
153 2013; Cavicchia et al., 2014a) or even less than one per year (Walsh et al., 2014; Tous and Romero,
154 2011).

155 In Miglietta et al. (2013), a combined satellite and modelling method has been used for obtaining a
156 list of the medicanes observed in different zones of the Mediterranean sea between 1999 and 2012,
157 and the difficulty of compiling a medicanes catalogue has been expressed. Note that the results in
158 Miglietta et al. (2013) are based on the analysis of individual case studies and cannot be considered
159 like a true climatological analysis. But the medicane detection method applied there is very similar
160 to the method used here, which makes this list particularly suitable for the RCM evaluation. Table 2
161 shows the medicanes frequency registered in that study and for the RCMs. Frequency values are
162 given for the whole Mediterranean Sea and for the three different subregions indicated above. In
163 addition to the annual values, monthly frequency from August to January is also shown. The

164 frequency of the medicanes studied by Miglietta et al. (2013) is 0.86 events/year for August-
 165 January, agreeing pretty well with the frequencies calculated in the other studies. According to
 166 Miglietta et al. (2013) the Central zone (between 10° and 24 ° E of longitude) is the region of the
 167 Mediterranean Sea with the largest number of detected medicanes, since half of them have been
 168 registered there, while the Eastern zone has only 0.14 events/year. Walsh et al. (2014) also pointed
 169 out the central zone of the Mediterranean Sea as the zone with a major risk of medicanes
 170 development, but Cavicchia et al. (2014a) indicated the western zone of the Mediterranean Sea as
 171 the zone with the strongest medicanes activity. According to Miglietta et al. (2013), taking into
 172 account the whole year, 85.7 % of the medicanes occurred from September to December, and more
 173 than one half occurred during the months of September and October. Nevertheless, Tous and
 174 Romero (2011) pointed out a different monthly distribution with the greatest number of medicanes
 175 in December. The different periods and methodologies used in the two studies are responsible for
 176 such discrepancies.

	Frequency	Distribution by			Distribution by months					
	(n/year)	regions (%)			(%)					
	Mediterranean	West	Center	East	Aug	Sep	Oct	Nov	Dec	Jan
Miglietta	0.86	33	50	17	0.0	33	33	17	17	0.0
RCA3	0.74	27.6	51.7	20.7	0.0	3.5	13.8	27.6	27.6	27.6
ALADIN	0.88	46	32.4	21.6	0.0	5.4	18.9	21.6	29.7	24.3
CLM	10.21	33.2	43.2	23.6	3.5	8.5	15.6	19.6	24.9	27.9
HadRM3Q16	2.02	19.3	54.2	26.5	2.4	3.6	12.1	26.5	27.7	27.7
HadRM3Q3	2.24	29.3	43.5	27.2	1.1	7.6	10.9	27.2	28.3	25
RACMO	2.48	27.9	51	21.1	3.9	6.7	11.5	26	26.9	25
HIRHAM	1.56	24.6	47.5	27.9	1.6	4.9	11.5	21.3	32.8	27.9

	Frequency	Distribution by			Distribution by months					
	(n/year)	regions (%)			(%)					
	Mediterranean	West	Center	East	Aug	Sep	Oct	Nov	Dec	Jan
REMO	1.67	27.7	44.6	27.7	3.1	0.00	9.2	30.8	23.1	33.8
RCA	0.67	42.3	42.3	15.4	0.00	0.00	19.2	30.8	23.1	26.9
PROMES	2.41	29.8	47.9	22.3	2.1	7.5	16	22.3	27.7	24.5
RCM Mean	2.49	30.4	45.6	24	2.6	6.5	13.9	23.3	26.5	27.2

177 Table 2: Annual frequency of medicanes for Miglietta et al. (2013) data, every RCM and RCMs mean for ERA40 period
178 (1961-2000): total frequency, regional relative frequency and monthly relative frequency. All data are calculated for
179 August to January.

180 The period to evaluate the ensemble of the ten ERA40-forced RCMs is from 1961 to 2000. Here we
181 compare the annual frequency from the ensemble with the results obtained in Miglietta et al. (2013).
182 The annual medicane frequency for most of the regional models ranges between 0.67 and 2.41, in
183 good agreement with previous studies (Romero and Emanuel, 2013; Cavicchia et al., 2014a; Walsh
184 et al., 2014; Tous and Romero, 2011). Only CLM presents a clear overestimation, with more than
185 10 events per year. CLM is the model which simulates the largest number of cyclones in general,
186 and more than 40 % of them are medicanes, which is clearly above the observed percentage. For the
187 rest of the models, the percentage of medicanes is less than 16 % of the total number of cyclones.
188 Regarding the distribution by regions, most of the models follow the observed distribution (with
189 maximum values over the Central part of the Mediterranean Sea), with the exception of ALADIN,
190 which simulates the western zone as the one with the largest number of medicanes, and RCA, with
191 an identical number of events in the western and in the central zone. With respect to the time
192 (monthly) distribution, most of the RCMs follows a similar behaviour, with the highest frequency in
193 November, December and January, showing a distribution closer to Tous and Romero (2011) than to
194 the results in Miglietta et al. (2013). Although the Tous and Romero (2013) and Miglietta et al.

195 (2013) databases show a decrease of medicanes activity during January, Cavicchia et al. (2014a)
196 detects a peak activity in that month. On the other hand, all models clearly underestimate the
197 relative frequency of medicanes in September. This may point to a common difficulty of the models
198 in representing early autumn medicanes, when the environmental factors favour only marginally
199 their formation.

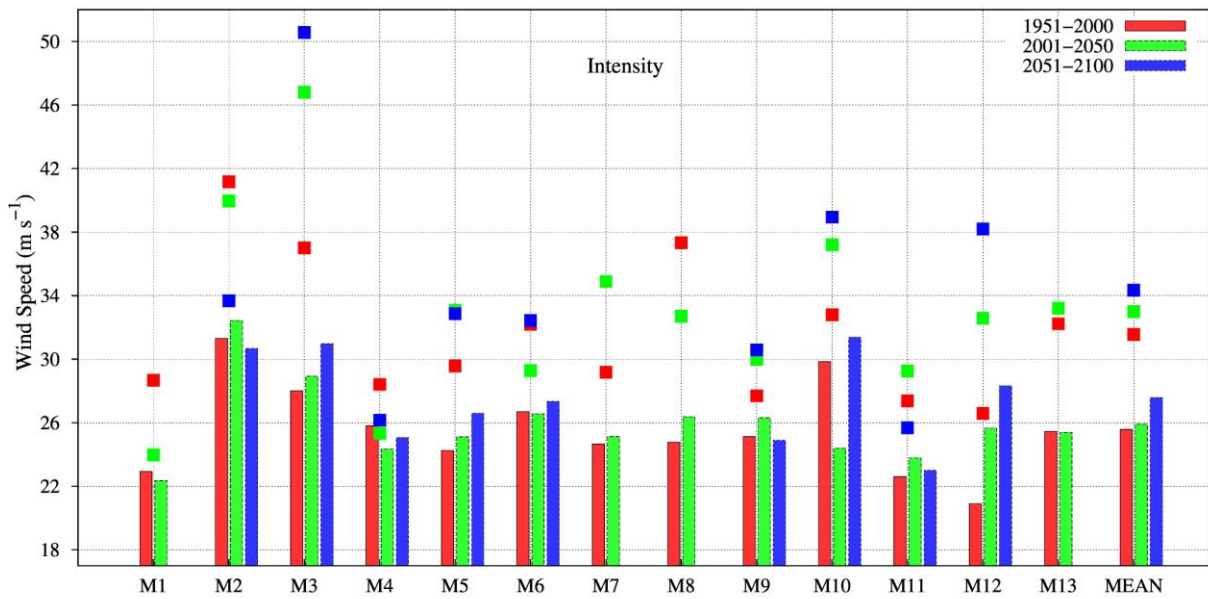
200 As explained above (section 1.2.2), the axial symmetry (B parameter) of the cyclones has not been
201 used to select the medicanes. But for the cases where B could be calculated, almost all of the
202 selected medicanes satisfy the axial symmetry criterion: eight of the ten RCMs simulate more than
203 93% of the medicanes with axial symmetry. CLM is the model with the least percentage of
204 symmetric medicanes (79,40%) followed by RCA3 (86,21%). The fact that the B parameter has not
205 been considered may partially explain the overestimation in the number of medicanes simulated by
206 CLM.

207 **1.3.2 Climate Change Projections (up to 2050 or 2100)**

208 In order to analyse the intensity extremes of the simulated medicanes, Figure 2 shows the 95th
209 percentile (p95, represented by colour bars) and the maximum value (represented by squares) of the
210 daily maximum wind speed near the centre of the medicanes for every RCM and every period
211 (1951-2000, 2001-2050 and 2051-2100; the latter period is not available for all models). The figure
212 shows a large variability among simulations, not only in the values of p95, but also in the tendency
213 in the future climate. This variability makes it difficult to find patterns common to different
214 simulations, but some interesting patterns can be identified. Looking at p95, six of the nine
215 simulations reaching 2100 show an extreme intensity increase from present climate to the second
216 half of XXIst century. This shows up clearly in the ensemble mean. Though the mean values
217 represented Figure 2 include all the simulations (thirteen for the first two periods), a very similar
218 increase is obtained including only the nine simulations covering also the third period, with p95
219 mean values of 26.06, 26.39 and 27.52 m·s⁻¹ for the respective periods. Previous studies, using one
220 only RCM, also concluded that the intensity extremes of the medicanes (Cavicchia et al., 2014a,

221 2014b) or of all Mediterranean cyclones (Lionello et al., 2002) will increase at the end of the
 222 century.

223 If we group the simulations by the driving GCM, some noteworthy results are obtained. Simulations
 224 nested in ECHAM (M1, M6, M9 and M11) show low to intermediate p95 values. These simulations
 225 show no clear tendency in intensity. In contrast to this, simulations nested in HCQ3 (M5, M12)
 226 show the clearest increasing tendency in intensity. Also two of the three simulations nested in
 227 HCQ0 present this upward tendency. The influence of the GCM can also be seen in the set of
 228 simulations with RCA, driven by different GCMs (M10-M12), with rather different p95 values and
 229 time dependence. Therefore, the GCM exerts a visible influence on the intensity values and
 230 tendency.

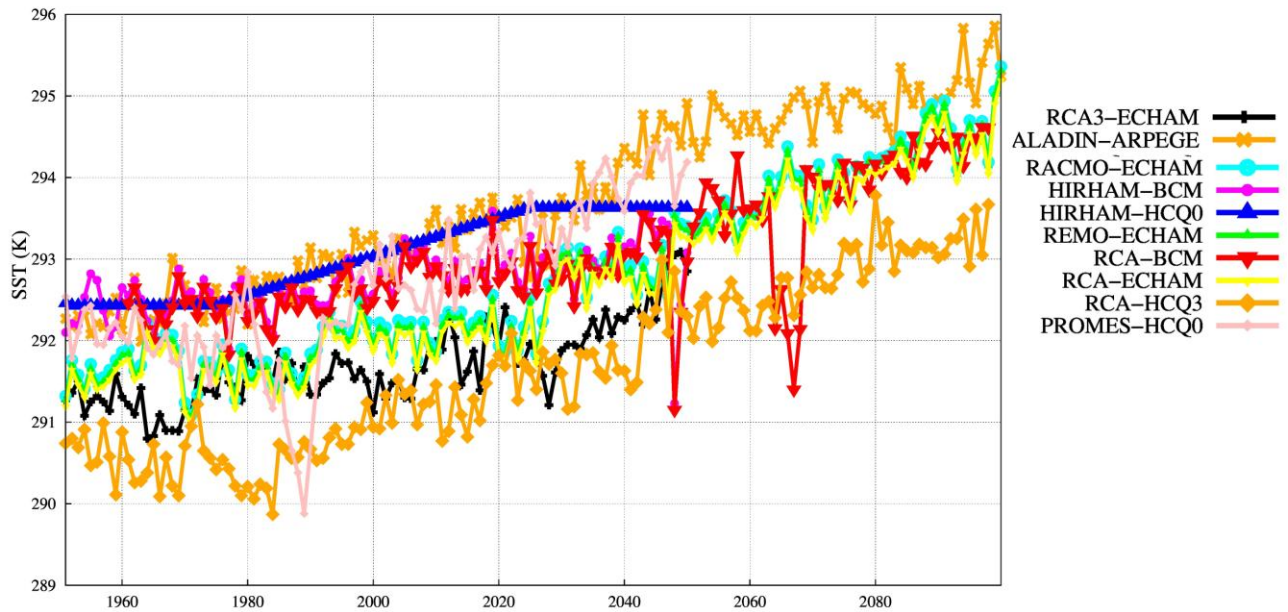


231 Figure 2: Wind Speed p95 ($\text{m}\cdot\text{s}^{-1}$) for all the RCMs and RCMs mean (MEAN) for the periods 1951-2000 (red bar),
 232 2001-2050 (green bar) and 2051-2100 (blue bar). Squares represent maximum wind speed for each model and period.
 233 Note that some RCMs simulations are available until 2050 so there is no blue bar neither blue square. In the figure
 234 M1=RCA3-ECHAM, M2=ALADIN-ARPEGE, M3=CLM-HCQ0, M4=HadRM3Q16-HCQ16, M5=HadRM3Q3-
 235 HCQ3, M6=RACMO-ECHAM, M7=HIRHAM-BCM, M8=HIRHAM-HCQ0, M9=REMO-ECHAM, M10=RCA-
 236 BCM, M11=RCA-ECHAM, M12=RCA-HCQ3 and M13=PROMES-HCQ0.

237

238 Maximum wind speed has also been depicted in Figure 2 (represented by colour squares) for each
239 simulation and period. Again, simulations nested in ECHAM (M1, M6, M9 and M11) give smaller
240 maximum wind values than the most of the other models. On the other hand, CLM-HCQ0 (M3)
241 stands out with the greatest maximum wind speed. The maximum wind speed shows a wider range
242 of values than p95. An increase in medicane intensity in future climate can also be drawn from this
243 variable, as summarised in the corresponding ensemble mean.

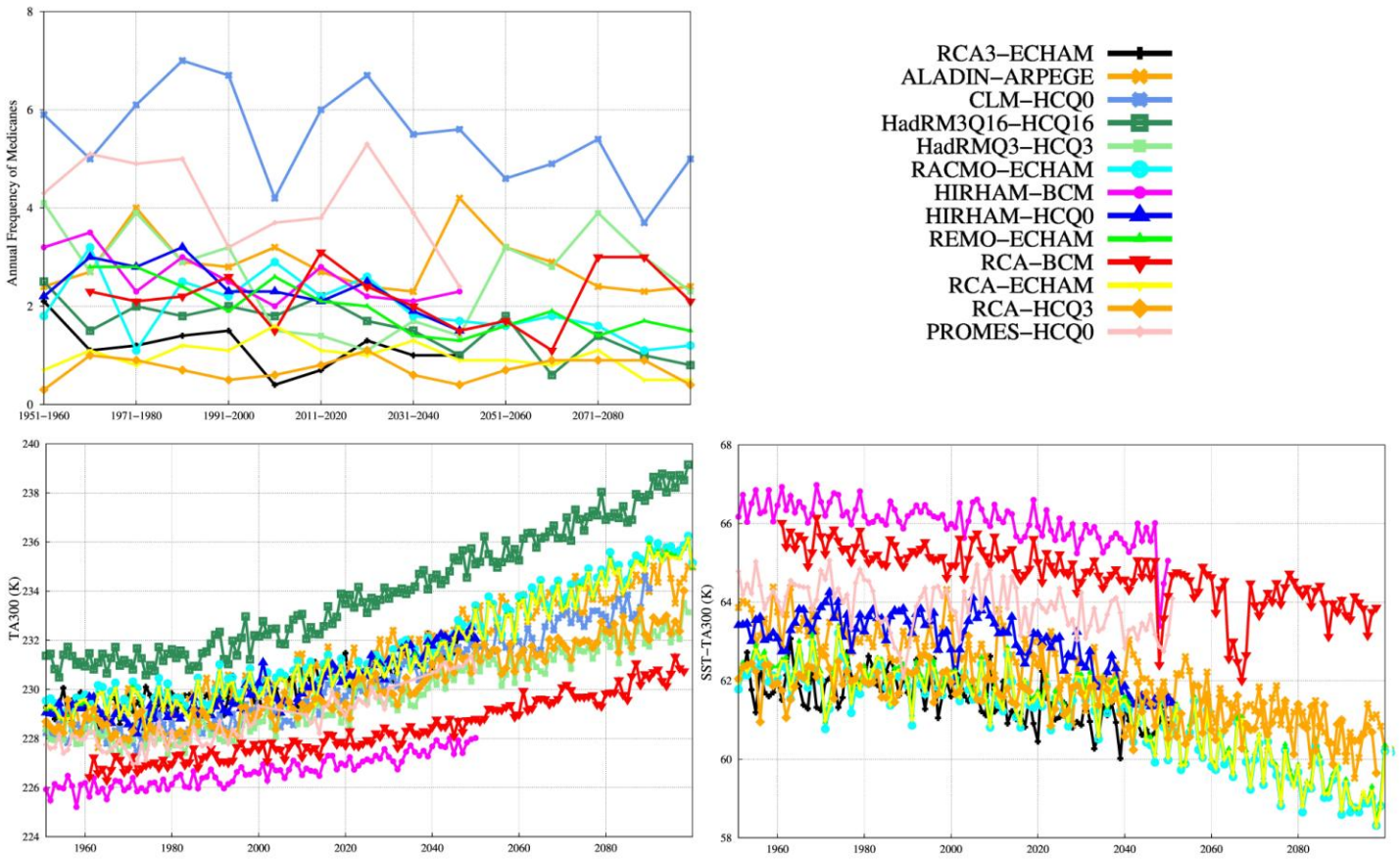
244 The increase in the medicane intensity extremes could be related to the projected increase in sea
245 surface temperature (SST). Once a medicane is formed, its intensity will depend on the available
246 energy which it can extract from the ocean through the Wind-Induced Surface Heat Exchange
247 (WISHE) mechanism (Rotunno and Emanuel, 1987), which strongly depends on enthalpy fluxes,
248 i.e. sensible and latent heat fluxes, and therefore on sea surface temperatures. Tous et al. (2013)
249 showed that air-sea interaction plays an important role for medicane development since cyclone
250 pressure minima and central pressure gradients were found to be undoubtedly influenced by surface
251 heat fluxes. Figure 3 shows how SST tends to rise in all simulations (note that for 3 simulations
252 there this variable was not available). Linked to this SST increase, the total surface heat flux (not
253 shown) also experiments an increase in ten of the thirteen models, driven by the increase in latent
254 heat flux. This should provide more available energy for the medicane intensification than in
255 present times.



256 Figure 3: Evolution of sea surface temperature (SST) for each of the simulations where it is available. As indicated
 257 before, some simulations end in 2050.

258

259 With respect to the projected changes in frequency, Figure 4 (top-left panel) shows the annual
 260 frequency of the medicanes from 1951 to 2100 for every simulation, averaged over each decade.
 261 Although the figure reflects an important decadal variability in the changes in the number of
 262 medicanes with time, there is an overall tendency to a decrease in the number of such events during
 263 the XXIst century. Eleven of the thirteen simulations have a negative slope, which is statistically
 264 significant for eight simulations at 95% confidence level, using a linear regression. Nevertheless,
 265 the result is less clear if we look only at the runs reaching 2100: less than half (four out of nine)
 266 show a statistically significant decrease. All three simulations with RCA regional model show no
 267 statistically significant change, with one of them showing no change and another one even an
 268 increase in medicane frequency. On the contrary, three of the four ECHAM-driven simulations
 269 show a statistically significant decrease. This points to a clear model dependency of the frequency
 270 decrease, and reinforces the need of considering simulation ensembles when these processes are
 271 studied.



273 Figure 4: Evolution of medicane decadal frequency (top-left), 300 hPa temperature (TA300) (bottom-left) and the
 274 difference between sea surface temperature (SST) and TA300 (bottom-right) for each model for the whole simulated
 275 period (1951-2100). Note that for some models simulations end in 2050.

276

277 The overall frequency decrease of medicanes and increase in their extreme intensity (Figure 2)
 278 under climate change conditions is consistent with the results from Walsh et al. (2014), Cavicchia et
 279 al. (2014a) and Romero and Emanuel (2013), although their methodology was different, as they
 280 used a single model or statistically based methods. Searching for a physical meaning, these changes
 281 could be related to differences in the evolution in the atmospheric and oceanic environment. As
 282 stated by Tous and Romero (2013), a necessary condition for a medicane development is the
 283 presence of a cut-off low in the upper-troposphere. Therefore, it is reasonable to hypothesize that a
 284 decrease in the number of medicanes will be linked to a decrease in the number of upper cut-off
 285 lows affecting the Mediterranean Basin.

286 Temperature at 300 hPa level (TA300) has been selected as proxy for the arrival of these cut-offs

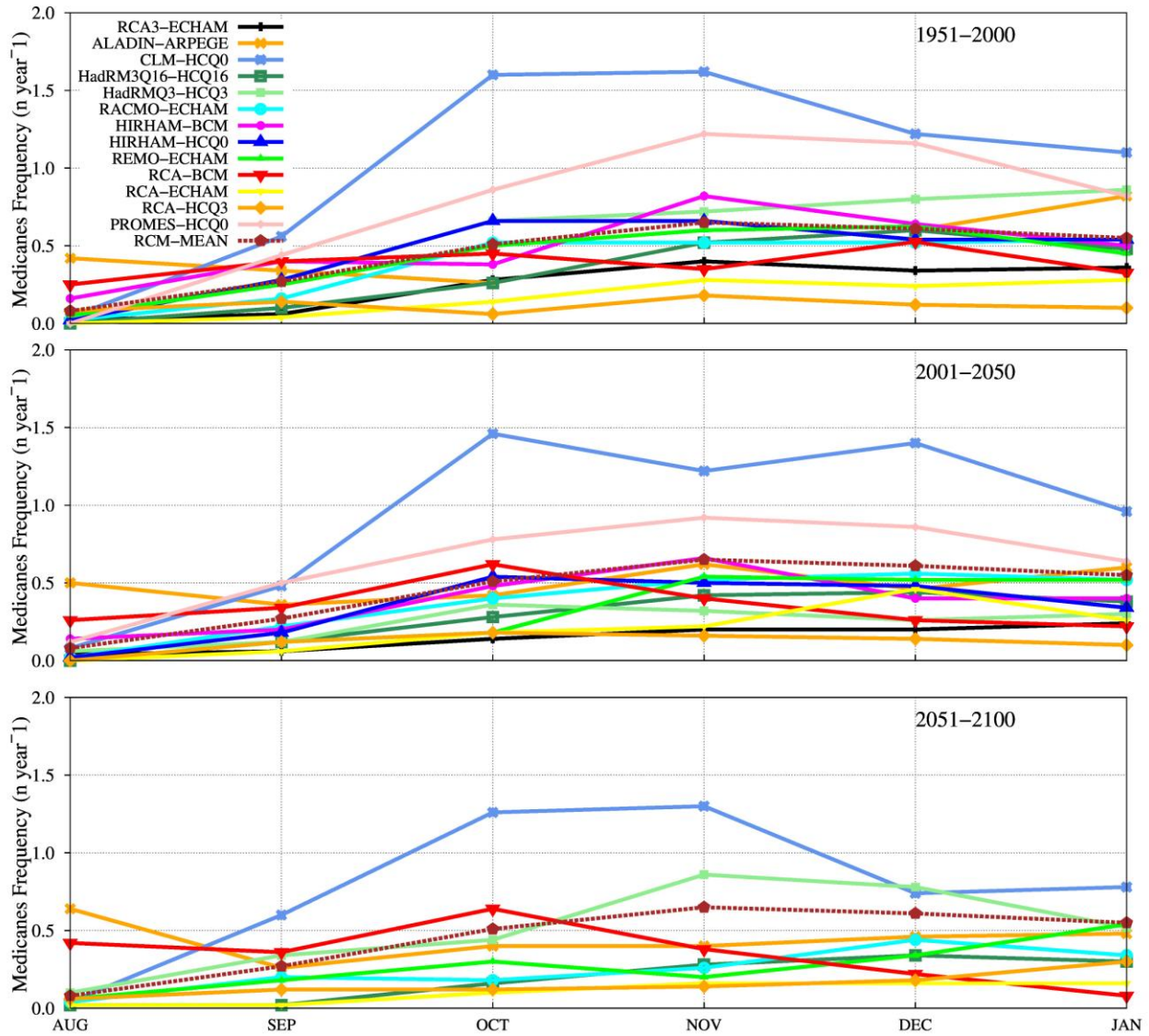
287 since they are associated with a drop in the temperature in the upper troposphere. Figure 4 (bottom-
288 left panel) shows that, in all models, there is a positive trend in TA300, statistically significant in
289 nine of the thirteen runs. This suggests that a decrease in the number of cut-offs affecting the
290 Mediterranean Sea could be expected in the future, and is consistent with projections of a poleward
291 movement of the mid-latitude storm track (Ulbrich and Christoph, 1999; Lionello et al., 2008;
292 Giorgi and Coppola, 2007). The lower frequency of cut-off lows reaching the Mediterranean Sea
293 would lead to changes in the vertical temperature difference between the surface and the upper
294 troposphere (a measure of static atmospheric stability), as is shown in Figure 4 (bottom-right panel).
295 All the simulations show indeed a positive trend for static stability, except for PROMES-HCQ0
296 (this simulation only reaches 2050). Note that lower values of the represented temperature
297 difference (SST-T300) indicate more stability. This average stability increase would cause
298 atmospheric environmental conditions to be worse for medicane development.

299 The highest values of static stability and the highest increase in it are found for ECHAM-driven
300 simulations. The same simulations show relatively low values of medicane frequency, as well as the
301 largest decrease in medicane frequency among the simulations running until 2100. This suggests a
302 relationship between average static stability and medicane frequency. The only partial exception to
303 this behaviour, among the four ECHAM-driven simulations, is the run with RCA in which the
304 frequency decreases only slightly and non-significantly. But this RCM shows the lowest frequency
305 values both in the scenario simulations and in the evaluation runs, and the low frequency values for
306 present climate obviously put a limit to the future decrease. It is also noteworthy that simulations
307 nested in ECHAM show relatively low intensity values, as shown before in Figure 2, which points
308 also to a relationship of this variable to static stability. Interestingly, the strong static stability
309 decrease for this GCM does not induce a decrease in extreme intensity in the future. On the other
310 hand, the lowest values of static stability are seen in BCM-driven simulations. The spread in static
311 stability between simulations increases from about 4 K in 1950 to about 5 K in 2100. This higher
312 spread is mainly due to the nearly constant value of static stability that RCA-BCM run reaches

313 during the last decades of the present century, which reflects in a clear pick-up of medicane
314 frequency in this run.

315

316 The monthly distribution of medicanes frequency (Figure 5) indicates that the spread among models
317 could decrease at the end of the century, although an important variability among runs remains. As
318 summarised by the ensemble mean (dashed line in the figures), no appreciable variations are
319 simulated in general under climate change conditions. An exception to this are RCA-BCM results,
320 as the monthly distribution in this simulation shifts from a December maximum in 1951-2000 to a
321 clear October maximum in 2051-2100. A marked future reduction in winter medicanes is seen in
322 this simulation, which also shows an appreciable increase in August medicanes. Similar changes are
323 also simulated by ALADIN-ARPEGE, which as a result shows an August maximum in 2051-2100.
324



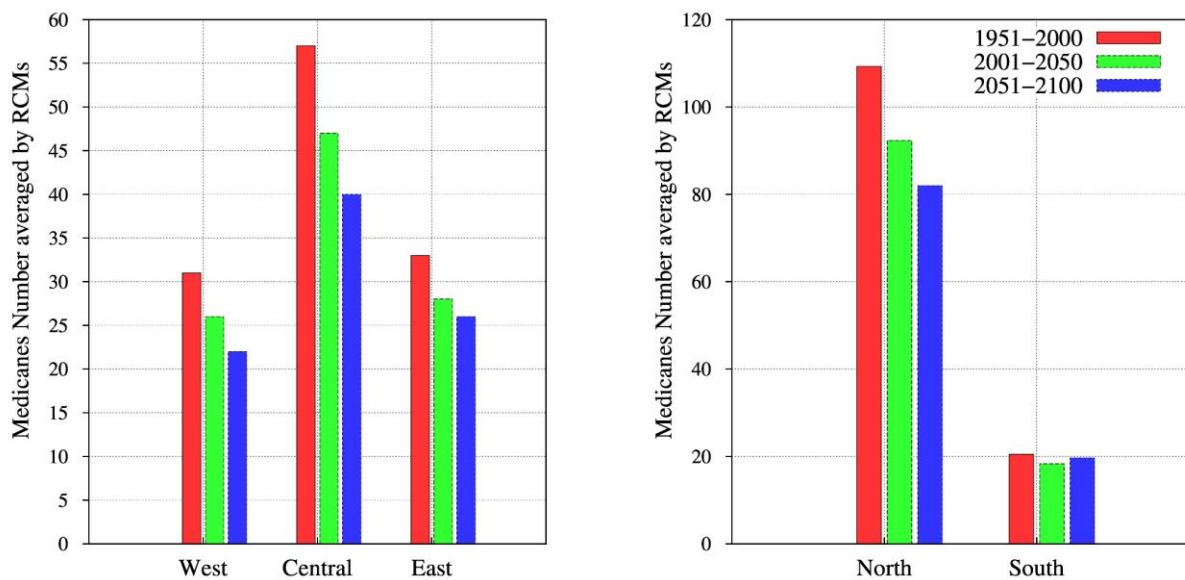
325 Figure 5: Monthly distribution of medicane frequency for every RCM, and RCM mean (dashed line), for every period:
 326 1951-2000 (top), 2001-2050 (middle) and 2051-2100 (bottom).

327

328 The total number of medicanes, divided by the number of available RCMs (thirteen up to 2050 and
 329 nine up to 2100), is represented in Figure 6, showing the regional distribution for each period. We
 330 assign each medicane to the region where it reaches its maximum 10 m wind speed. The left panel
 331 shows the distribution following the regions defined in Figure 1. A decrease in the number of
 332 medicanes at the end of the century is clearly identified over the whole Mediterranean Sea,
 333 independently of the region. As Miglietta et al. (2013) have pointed out, the central region of the
 334 Mediterranean Sea is the region which presents the largest number of medicanes, and this result
 335 persists under climate change conditions. But this central region will suffer a larger decrease than

336 the other areas in future climate.

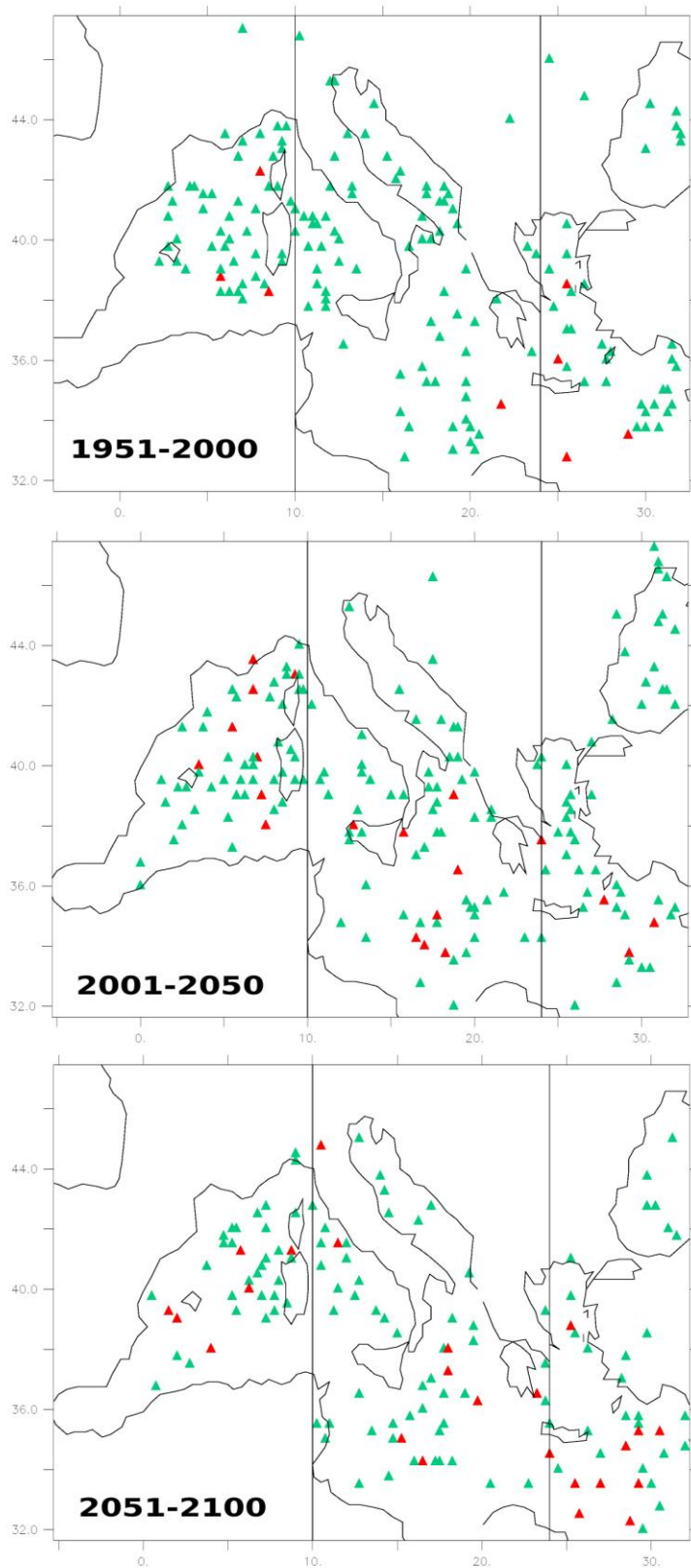
337 The right panel of figure 6 shows a different regional distribution, dividing the Mediterranean Sea
338 in two zones, north and south of 36°N. The greater number of medicanes appear in the north of
339 Mediterranean Sea, but the number of events is projected to decrease there under climate change
340 conditions. In contrast, the southern part of the Mediterranean Sea is the only place where the
341 number of medicanes should not experience any change in the future. According to Figure 6 (left
342 and right panels) the regions with a larger number of medicanes in the first period will suffer a more
343 pronounced decrease in the future so the number of medicanes will be distributed in a more uniform
344 way along the Mediterranean Sea at the end of the century.



345 Figure 6: Regional distribution of total number of medicanes, divided by the 13 RCMs available up to 2050 and by 9
346 RCMs available up to 2100, for each region (left: west, central and east according to Figure 1; right: north, for latitude
347 greater than 36°N, and south, for latitude less than 36°N) and for each period: 1951-2000 (red), 2001-2050 (green) and
348 2051-2100 (blue).

349
350 In figure 7 all the detected medicanes, no matter from which RCM simulation they come from, with
351 maximum surface wind speed above $25 \text{ m} \cdot \text{s}^{-1}$ during their lifetime (threshold between strong gale
352 force and storm force in Beaufort Scale) are represented. The green colour indicates maximum

353 surface wind speed between 25 and 33 m·s⁻¹ (minimum threshold of Saffir-Simpson Hurricane
354 Wind Scale) while red colour represents the most intense medicanes (maximum wind speed higher
355 than 33 m·s⁻¹, i.e. hurricane strength). The zones with the highest number of medicanes are Ligurian
356 Sea (North of Corsica), Tyrrhenian Sea, Adriatic Sea, the Balearic Sea, the Ionian Sea and Aegean
357 Sea in the first (1951-2000) and second (2001-2050) modelled periods. But in the far future climate
358 (2051-2100) the medicanes seem to be distributed all over the Mediterranean Sea in a more
359 homogeneous way. As previously discussed with respect to Figure 2, the intensity of the strongest
360 medicanes should increase in future climate (more red points in the last period). Figure 7 shows that
361 an important fraction of the most intense medicanes could form in the southern and eastern parts of
362 the Mediterranean Sea, in the regions where the number of events is more scarce in general. The
363 maximum SSTs in the Mediterranean Sea are found precisely over these parts, which points to a
364 important role of the projected SST increase in the increased extreme intensity of medicanes.



365 Figure 7: Scatter plot of the medicanes occurrence for 1951-2000 (top), 2001-2050 (middle) and 2051-2100 (bottom).
 366 The colours represent the maximum value of surface wind speed along the whole life of the medicane: green points
 367 represent wind speed between 25 and 33 $\text{m}\cdot\text{s}^{-1}$ and red points represent wind speed greater than 33 $\text{m}\cdot\text{s}^{-1}$. Medicanes
 368 with smaller values of maximum daily wind speed have not been represented.
 369 The total number of medicanes simulated in each run for the three analysed periods is listed in Table

370 3, where the medicanes are classified in three groups according to their maximum intensity:
371 between 17 and 25 m·s⁻¹, between 25 and 33 m·s⁻¹ (intense) and greater than 33 m·s⁻¹ (very
372 intense). All runs simulate a decrease in the number of medicanes with intensity between 17 and 25
373 m·s⁻¹ with the only exception of RCA-BCM, in agreement with previously shown results for the
374 overall medicane number tendency. For the intense and very intense medicanes there is no common
375 tendency, as the variability among the simulations is very important. The strong influence of the
376 GCM on the results can be seen in the ECHAM-driven simulations, which do not generate any very
377 intense medicanes, and in the three simulations with RCA regional model nested in different GCMs,
378 which show very different evolutions of the three types of medicanes. It is noteworthy that two of
379 the three runs that generate hurricane-force medicanes in the second half of present century (RCA-
380 BCM and ALADIN-ARPEGE) show an appreciable increase in August medicanes (see Figure 5),
381 which suggests a possible relationship to the yearly SST maximum in that month. A summary of the
382 ensemble results is shown in the last row of Table 3, where the mean number of medicanes for all
383 the simulations reveals a decrease in the number of medicanes with maximum wind speed between
384 17 and 25 m·s⁻¹ and an increase in the number of both intense and very intense events under future
385 climate change conditions.

386

	1951-2000			2001-2050			2051-2100		
Maximum daily Wind Speed (m·s⁻¹)	17-25	25-33	>33	17-25	25-33	>33	17-25	25-33	>33
RCA3-ECHAM	70	3	0	44	0	0	-	-	-
ALADIN-ARPEGE	93	0	0	59	24	5	51	14	3
CLM-HCQ0	258	45	4	223	48	9	178	47	11
HadRM3Q16-HCQ16	89	9	0	80	2	0	52	4	0
HadRM3Q3-HCQ3	161	7	0	66	4	1	139	13	0

RACMO-ECHAM	104	10	0	100	12	0	65	8	0
HIRHAM-BCM	139	6	0	107	6	1	-	-	-
HIRHAM-HCQ0	128	6	1	96	7	0	-	-	-
REMO-ECHAM	92	7	0	80	14	0	76	5	0
RCA-BCM	50	6	0	71	4	1	70	7	5
RCA-ECHAM	31	1	0	37	2	0	18	2	0
RCA-HCQ3	161	7	0	66	4	1	139	13	0
PROMES-HCQ0	211	14	0	177	13	1	-	-	-
RCM MEAN	122,1	9,3	0,4	92,8	10,8	1,5	87,6	12,6	2,1

387 Table 3: Total number of medicanes for every RCM and RCM mean (rows) and period (columns). The number of
388 medicanes are classified according to their maximum daily value of surface wind speed: between 17 and 25 m·s⁻¹,
389 between 25 and 33 m·s⁻¹ and greater than 33 m·s⁻¹.

390 1.4 Conclusions

391 Several previous studies have dealt with the analysis of medicanes in the present and future climate
392 using single climate model simulations. In order to overcome the limitations of such a single model
393 approach, here an ensemble of ten RCMs from ENSEMBLES project is used to study the
394 occurrence of medicanes (tropical-like cyclones) over the Mediterranean Sea in the present climate
395 and the changes of this kind of events in future climate conditions for the whole XXIst century. The
396 aim is to advance previous studies along several important lines: use of a large ensemble of RCMs,
397 nested in many different GCMs, and covering a continuous long time period (up to 150 years). An
398 objective method, using a cyclone tracking method (Picornell et al., 2001) and studying the vertical
399 structure of the cyclones through the cyclone phase space method of Hart (2003), has been
400 employed to identify and define each medicane event.

401 First, the ERA40-forced evaluation runs (1961-2000) have been compared with a list of observed
402 medicanes (Miglietta et al., 2013) in order to evaluate the capability of the RCMs to simulate

403 several observed characteristics of medicanes. Almost all RCMs obtain frequency values between
404 0.7 and 2.5 medicanes per year, which compares well with the available information from several
405 observational datasets. The important variability among the RCMs is comparable to the spread
406 among available observational datasets. Other characteristics of observed medicanes are reasonably
407 well reproduced by the RCMs.

408 As some RCMs have been nested in different GCMs, an ensemble of thirteen simulations (four
409 covering the period 1950-2050 and nine extending to 2100) has been used to study the projected
410 changes in medicanes under future climate change conditions. The two main results are a decrease
411 in the number of medicanes per year and an increase in the extreme intensity of such events during
412 the XXIst century. These results are consistent with those emerging in recent studies using one
413 model (e.g., Cavicchia et al., 2014a, 2014b; Walsh et al., 2014) or a statistically based method
414 (Romero and Emanuel, 2013). Nevertheless, our approach reveals interesting uncertainties in these
415 results. The frequency decrease is less clear if we take into account only the runs reaching 2100:
416 less than half (four out of nine) show a statistically significant decrease. There is a clear dependency
417 on the model formulation in this decrease. Regarding the projected intensity changes, some
418 systematic patterns are also apparent: ECHAM-driven runs simulate less intense medicanes in
419 general, while the simulations nested in HCQ3 GCM show the clearest increasing tendency in
420 intensity.

421 No clear future changes are found in the monthly distribution of medicanes, but again a few
422 noticeable exceptions are seen, as in two simulations a shift towards an earlier monthly maximum is
423 obtained, together with an increase in August medicanes. On the other hand, the projected decrease
424 in medicanes shows some dependence on the spatial distribution. The central zone of the
425 Mediterranean Sea, which presently is the subregion with a larger number of events, will experience
426 a larger decrease than the western and eastern zones. Remarkably, when the Mediterranean Sea is
427 divided into northern and southern subregions, no future medicane decrease is identified in the
428 southern part, in clear contrast to the northern part. At the same time, the extreme intensity of

429 medicanes is projected to increase more clearly in the southern part.

430 In order to find physical explanations for the projected tendencies and the differences among
431 simulations, some environmental variables have been explored. A general increase with time of the
432 vertical static stability of the atmosphere seems a plausible reason for the overall decrease of
433 medicane frequency. Some differences among models seem to be linked to static stability, as
434 ECHAM-driven simulations show the highest overall values of static stability and the highest future
435 increase in it. As the same simulations show relatively low values of medicane frequency, as well as
436 the largest projected decrease in it, a link between medicane frequency and average static stability
437 is suggested. A rather large spread is found for this environmental variable. This could explain
438 partly the differences among simulations. It is noteworthy that the clear increase in average static
439 stability projected for the end of present century is not enough to avoid that the most intense
440 medicanes show higher maximum winds in many of the projections. It is likely that the increased
441 SST and latent heat fluxes can overcome this limitation in the atmospheric situations where
442 favourable conditions for medicane genesis indeed occur. This is a matter of concern, as the
443 strongest negative impacts are associated to the most intense cyclones.

444 As more regional dynamical simulations are becoming available in ongoing projects, this
445 methodology and analysis is expected to be tested for higher resolution and even coupled
446 atmosphere-ocean regional simulations, to see if these results can be confirmed and the
447 characteristics of these important extreme cyclones over the Mediterranean can be further
448 understood and analysed by means of RCMs.

449

450 **1.5 Acknowledgements**

451 This work has been funded by the grant CGL2010-18013 (Spanish Ministry of Science and
452 Innovation) and grant CGL2013-47261-R (Spanish Ministry of Economy and Competitiveness), and
453 by ESCENA project (Ref: 200800050084265, Spanish Ministry of Environment and Rural and

454 Marine Affairs). These projects have been co-funded by the European Regional Development Fund.

455 1.6 References

456 Bocheva L, Georgiev CG, Simeonov P (2007) A climatic study of severe storms over Bulgaria
457 produced by Mediterranean cyclones in 1990-2001 period. *Atmos Res*, 83: 284-293,
458 doi:10.1016/j.atmosres.2005.10.018

459 Campins J, Genovés A, Picornell MA, Jansà A (2011) Climatology of Mediterranean cyclones using
460 the ERA-40 dataset. *Int J Climatol*, 31: 1596-1614, doi: 10.1002/joc.2183

461 Christensen JH, Christensen OB (2007) A Summary of the PRUDENCE Model Projections of
462 Changes in European Climate by the end of this century. *Climatic Change*, 81, 1: 7-30, doi:
463 10.1007/s10584-006-9210-7

464 Cavicchia L, von Storch H (2012) The simulation of medicanes in a high-resolution regional
465 climate model. *Clim Dyn*, 39: 2273-2290, doi: 10.1007/s00382-011-1220-0

466 Cavicchia L, von Storch H, Gualdi S (2014a) A long-term climatology of medicanes. *Clim Dyn*, 43:
467 1183-1195, doi: 10.1007/s00382-013-1893-7

468 Cavicchia L, von Storch H, Gualdi S (2014b) Mediterranean tropical-like cyclones in present and
469 future climate. *J Climate*, 27: 7493-7501, doi: 10.1175/JCLI-D-14-00339.1

470 Christensen JH, Kumar KK, Aldrian E, An S-I, Cavalcanti IFA, de Castro M, Dong W, Goswami P,
471 Hall A, Kanyanga JK, Kitoh A, Kossin J, Lau N-C, Renwick J, Stephenson DB, Xie S-P, Zhou T
472 (2013). Climate Phenomena and their Relevance for Future Regional Climate Change. In: *Climate*
473 *Change 2013: The Physical Science Basis. Contribution of Working Group I to the Fifth*
474 *Assessment Report of the Intergovernmental Panel on Climate Change* [Stocker TF, Qin D, Plattner
475 G-K, Tignor M, Allen SK, Boschung J, Nauels A, Xia Y, Bex V, Midgley PM (eds.)]. Cambridge
476 University Press, Cambridge, United Kingdom and New York, NY, USA

477 Gaertner MA, Jacob D, Gil V, Domínguez M, Padorno E, Sánchez E, Castro M (2007) Tropical
478 cyclones over the Mediterranean Sea in climate change simulations. *Geophys Res Lett*, 34(14):

479 L14711, doi: 10.1029/2007GL029977

480 Giorgi F, Coppola E (2007) European climate-change oscillation (ECO). *Geophys Res Lett*, 34:
481 L21703

482 Giorgi F, Lionello P (2008) Climate change projections for the Mediterranean region. *Global Planet*
483 *Change*, 63(2): 90-104

484 Hart R (2003) A cyclone phase space derived from thermal wind and thermal asymmetry. *Mon.*
485 *Wea. Rev.*, 131: 585-616

486 Jansà A, Genovés A, Picornell MA, Campins J, Riosalido R, Carretero O (2001) Western
487 Mediterranean cyclones and heavy-rain. Part 2: Statistical approach. *Meteorol Appl*, 8(1): 43-56

488 Lionello P, Dalan F, Elvini E (2002) Cyclones in the Mediterranean region: the present and the
489 doubled CO₂ climate scenarios. *Clim Res*, 22: 147-159

490 Lionello P, Boldrin U, Giorgi F (2008a) Future changes in cyclone climatology over Europe as
491 inferred from a regional climate simulation. *Clim Dyn* 30: 657-671. Doi: 10.1007/s00382-007-
492 0315-0

493 Miglietta MM, Laviola S, Malvaldi A, Conte D, Levizzani V, Price C (2013) Analysis of
494 tropical-like cyclones over the Mediterranean Sea through a combined modeling and satellite
495 approach. *Geophys Res Lett*, 40(10): 2400-2405, doi: 10.1002/grl.50432

496 Nissen KM, Leckebusch GC, Pinto JG, Renggli D, Ulbrich S, Ulbrich U (2010) Cyclones causing
497 wind storms in the Mediterranean: characteristics, trends and links to large-scale patterns. *Nat*
498 *Hazards Earth Syst Sci*, 10: 1379-1391, doi:10.5194/nhess-10-1379-2010

499 Picornell MA, Jansà A, Genovés A, Campins J (2001) Automated database of mesocyclones from
500 the HIRLAM-0.5 analyses in the western Mediterranean. *Int J Climatol*, 21: 335-354

501 Pinto JG, Spanghel T, Ulbrich U, Speth P (2005). Sensitivities of a cyclone detection and tracking
502 algorithm: individual tracks and climatology. *Meteorologische Zeitschrift*, 14(6), 823-838.

503 Romero R, Emanuel K (2013) Mediane risk in a changing climate. *J Geophys Res-Atmos*, 118:
504 5992-6001, doi: 10.1002/jgrd.50475

505 Rotunno R, Emanuel K (1987) An air-sea interaction theory for tropical cyclones. Part II:
506 Evolutionary study using a nonhydrostatic axisymmetric numerical model. *J Atmos Sci*, 44: 542-
507 561

508 Sinclair M (1997) Objective identification of cyclones and their circulation intensity, and
509 climatology. *Weather Forecast*, 12: 595-612

510 Trigo IF, Davies TD, Bigg GR (2000) Decline in Mediterranean rainfall caused by weakening of
511 Mediterranean cyclones. *Geophys Res Lett*, 27: 2913-1916

512 Tous M, Romero R (2011) Medicanes: cataloguing criteria and exploration of meteorological
513 environments. *Tethys*, 8: 53-61. doi: 10.3369/tethys.2011.8.06

514 Tous M, Romero R (2013) Meteorological environments associated with medicane development.
515 *Int J Climatol*, 33: 1-14

516 Tous M, Romero R, Ramis C (2013) Surface heat fluxes influence on medicane trajectories and
517 intensification. *Atmos Res*, 123: 400-411

518 Ulbrich U, Christoph M (1999) A shift in the NAO and increasing storm track activity over Europe
519 due to anthropogenic greenhouse gas. *Clim Dyn*, 15: 551-559

520 Van der Linden P, Mitchell JFB (2009) ENSEMBLES: Climate Change and its Impacts: Summary
521 of Research and Results from the ENSEMBLES Project. *Mediterranean...* Vol 160
522 [http://ensembles-](http://ensembles-eu.metoffice.com/docs/Ensembles_final_report_Nov09.pdf)
523 [eu.metoffice.com/docs/Ensembles_final_report_Nov09.pdf](http://onlinelibrary.wiley.com/doi/10.1002/9781119941156.ch9/summary)
524 [/10.1002/9781119941156.ch9/summary](http://onlinelibrary.wiley.com/doi/10.1002/9781119941156.ch9/summary).

525 Walsh K, Giorgi F, Coppola E (2014) Mediterranean warm-core cyclones in a warmer world. *Clim*
526 *Dyn*, 42: 1053-1066. doi: 10.1007/s00382-013-1723-y